

# LHTES

Subjects: **Energy & Fuels**

Contributor: Saeed Tiari

Latent heat thermal energy storage systems (LHTES) are useful for solar energy storage and many other applications, but there is an issue with phase change materials (PCMs) having low thermal conductivity. This can be enhanced with fins, metal foam, heat pipes, multiple PCMs, and nanoparticles (NPs). This entry focuses on nano-enhanced PCM (NePCM) alone and with additional enhancements. Low, middle, and high temperature PCM are classified, and the achievements and limitations of works are assessed. The review is categorized based upon enhancements: solely NPs, NPs and fins, NPs and heat pipes, NPs with highly conductive porous materials, NPs and multiple PCMs, and nano-encapsulated PCMs. Both experimental and numerical methods are considered, focusing on how well NPs enhanced the system. Generally, NPs have been proven to enhance PCM, with some types more effective than others. Middle and high temperatures are lacking compared to low temperature, as well as combined enhancement studies. Al<sub>2</sub>O<sub>3</sub>, copper, and carbon are some of the most studied NP materials, and paraffin PCM is the most common by far.

latent heat thermal energy storage

phase change material

nanoparticles

nano-enhanced PCM

## 1. Introduction to Latent Heat Thermal Energy Storage

Solar energy is a great renewable energy alternative; however, it is an intermittent energy source. At night and on overcast days, solar energy is not available. This can be solved with the use of latent heat thermal energy storage (LHTES) systems, which are dispatchable. LHTES systems rely on phase change material (PCM) to charge and discharge energy in the form of heat by melting and solidification. LHTES systems can be anything from a simple container of PCM to complex systems with various enhancements. PCM is any material that can store energy through melting and release it upon solidification. This stored energy can be dispatched in the off hours to keep a system running.

LHTES systems are just one type of thermal energy storage. Other types include sensible heat storage (SHS) and thermo-chemical storage (TCS). TCS uses materials that store and release energy through endothermic and exothermic reactions, which are called thermo-chemical materials. Some examples of these materials are potassium oxide and lead oxide. Heat is applied to the material, which breaks into two parts that are separately stored. To release the energy, they are mixed back together. This process is shown in **Figure 1c**. SHS uses storage media such as water, sand, or rocks to store thermal energy. The most common being water. SHS is

popular because it is cheap and safe, using non-toxic materials. Temperature change is what drives SHS, as shown in **Figure 1a** [1].

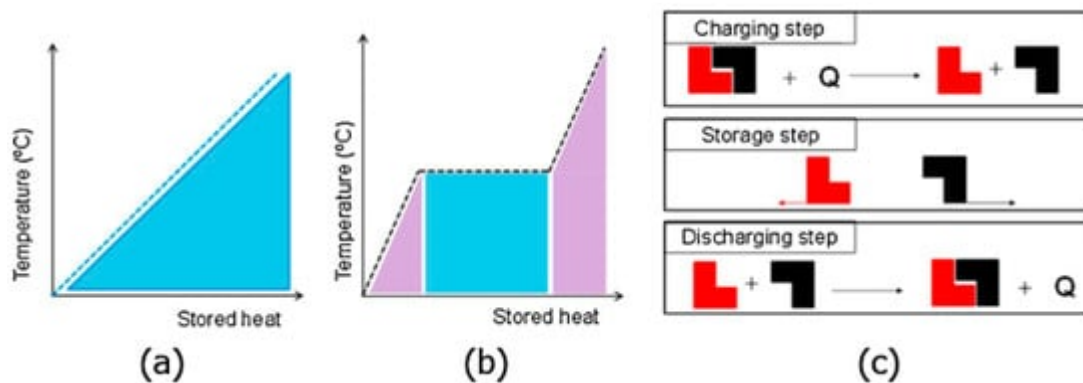


**Figure 1.** (a) Sensible heat, (b) latent heat, (c) thermo-chemical thermal energy storage systems (Copyright 2015 Gracia and Cabeza) [2].

SHS is the most common method, but latent heat is even more promising. The higher thermal storage density, large array of PCMs, and nearly isothermal behavior of LHTES systems (shown in **Figure 1b**) make them more convenient than the other methods [3]. This means that LHTES systems can take up less volume to store the same amount of energy as SHS, and the stable temperature allows nearly isothermal heating/cooling [1]. They also only require one sealed container and do not need salt pumps, transport lines, or heat tracing and operate at a wide range of temperatures depending on the PCM [4]. However, there are some disadvantages: the initial cost is higher, and PCMs have a higher risk of leaking [4].

## 1.1. Applications of LHTES Systems

LHTES systems have a wide array of applications that span across many different fields. They can aid in both heating and cooling systems, as well as energy storage, which can be converted to electrical energy. Some cooling applications include electronic cooling, air conditioning, refrigeration systems [4], lithium-ion battery cooling [5][6], and cold food packaging [6]. Some heating applications include building heating [4], waste heat recovery (for example, car exhaust, factories) [4][7] and solar food drying equipment [4].

One general energy storage application is solar power storage, which includes concentrated solar power (CSP) generation systems [7]. Even some medical applications exist, including smart textiles, which can work to either heat or cool the person depending on the need [6].

## 1.2. Types of PCM

PCMs can be characterized as low, middle, or high melting temperature. The potential applications of a PCM depend on its melting point, making this an important characteristic. According to Huang et al., middle temperature PCMs can be defined as those that melt between 120 and 300 °C, putting low temperature below 120 °C and high temperature above 300 °C [8]. Therefore, this paper will characterize low, middle, and high temperature PCMs

according to these ranges. The following will discuss several types of PCM, all of which have a variety of melting temperatures.

## 2. Nano-Enhanced PCM

### 2.1. Nanoparticles as Sole Enhancement

Elgafy and Lafdi in 2005, to the authors' best knowledge, were one of the first to study NePCMs. They experimentally and analytically studied paraffin wax enhanced with carbon nanofibers. Thermophysical properties and temperatures during solidification were recorded for different carbon nanofiber mass ratios, and the analytical model was used to predict effective thermal conductivity. The laser flash technique was used to measure thermal diffusivities. Thermal diffusivity increased with the increase in carbon fibers; however, the specific heat decreased. Increasing the carbon nanofibers decreased the solidification time of the NePCM and increased the output power. The analytical solution was compared to the experimental results with good agreement. Modifying the nanofibers surfaces also increased the solidification rate [\[9\]](#).

#### 2.1.1. Water NePCMs with Cu

Khodadadi and Hosseinizadeh were among the first researchers to study NePCMs, with their numerical model for water PCM enhanced with copper NPs. They studied the influence dispersion of NPs on the thermal conductivity, solidification rate, and latent heat of fusion. The latent heat of fusion was lowered, the rate of heat release was increased, and thermal conductivity was enhanced with the addition of NPs. It was concluded that NePCM was promising for thermal energy storage applications [\[10\]](#). Jourabian and Farhadi also numerically studied the melting of ice as a PCM enhanced with copper NPs enclosed in a vertical semicircle enclosure. Different Rayleigh numbers were tested, showing that this parameter's increase strengthens buoyancy-driven convection. The NePCM was also compared to pure PCM at three Rayleigh numbers. The NPs increased the temperature of the PCM, which is an effect that increased with Rayleigh's number. NPs provided more enhancement at lower Rayleigh numbers, but there were higher melting rates at higher Rayleigh numbers. The NPs increased the thermal conductivity and decreased the latent heat of fusion. The effect of the NPs on the Nusselt number was considered to be negligible [\[11\]](#). Another study using water PCM [\[12\]](#) numerically investigated enhancement with copper NPs. An LBM was developed and used to study how NP volume fraction and Grashof number affected heat transfer and the flow structure in NePCM. Higher Grashof numbers caused different, asymmetric convection patterns depending on the NP volume fraction. The local Nusselt number decreased with the increase in NP volume fraction, which is a result of higher thermal conductivity. Heat transfer efficiency was improved with the addition of NPs, and a higher volume fraction caused faster temperature change and melting. Energy storage was also increased with volume fraction. The copper NPs clearly enhanced the PCM melting process [\[12\]](#).

#### 2.1.2. Paraffin and Alumina

Paraffin wax and paraffin-based PCMs are a popular choice, and with a wide range of low temperature melting points and compatibility with different types of NPs, they are very important to study. Akhmetov et al. [\[13\]](#) used

COMSOL Multiphysics to numerically study two LHTES systems using two paraffin wax PCMs with low (PW-L) and high (PW-H) phase change temperatures.  $\text{Al}_2\text{O}_3$  NPs were used to increase the heat transfer in the system. Temperature-dependent properties were used in the three-dimensional simulations. They created three mixtures for each type of wax: pure wax, 2 wt % NP, and 4 wt % NP. These mixtures were used to measure and calculate thermal and physical properties for use in the simulations. The LHTES systems were set up sequentially, with the PW-H LHTES receiving heat first and then the PW-L LHTES receiving heat. Both types of paraffin had low thermal conductivities, which were improved by the addition of the  $\text{Al}_2\text{O}_3$  NPs. The LHTES system (shown in **Figure 2**) was determined to distribute energy efficiently and uniformly to the PCM containers as individual storage units. The sequential nature of the two LHTES systems was also effective [13].

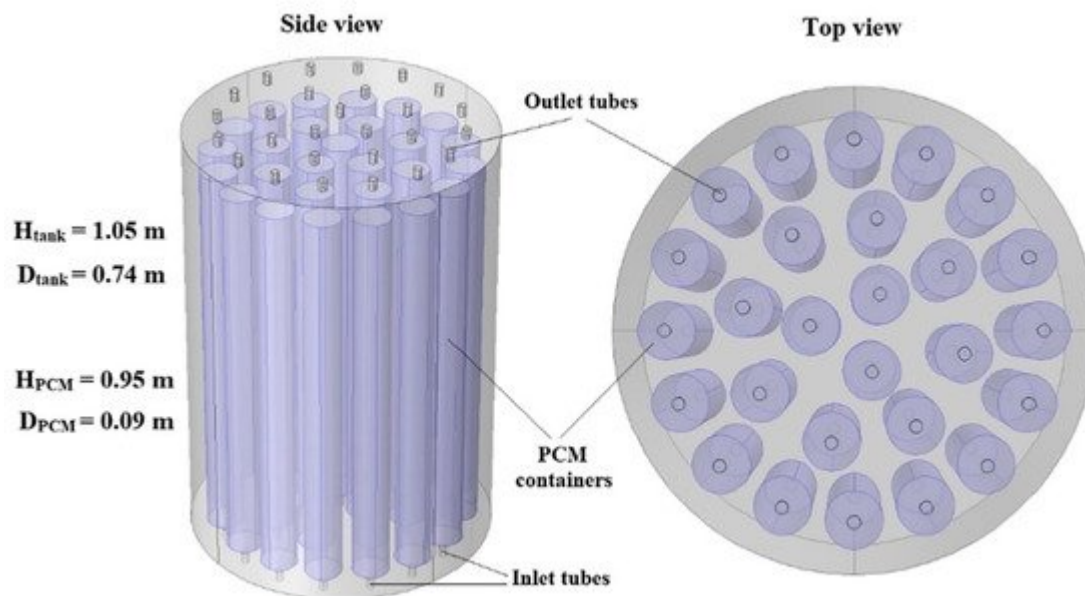


**Figure 2.** LHTES system configuration for the study by Akhmetov et al. (Copyright 2019 International Solar Energy Society) [13].

As in the previous study, alumina was used in many different studies as the NP enhancement for paraffin. Abdulateef et al. [14] numerically and experimentally studied a triplex tube heat exchanger LHTES system with RT82 PCM and alumina NPs. The heat exchanger had inner and outer tubes with HTF, and a middle tube of PCM with eight equally spaced fins. The numerical study tested longitudinal and triangular fins in the same heat exchanger. The experimental results showed that the internal heating method did not fully charge the PCM, while the external heating fully melted the RT82 at a lower HTF temperature and time. The ideal HTF mass flow rate was determined to be 29.4 kg/min. The numerical study showed that the triangular fins resulted in a faster melting process, and the addition of NPs further improved the system [14].

Zaidan and Alhamdo [15] studied a waste heat recovery system with paraffin PCM enhanced with  $\text{Al}_2\text{O}_3$  NPs at different volume fractions both experimentally and numerically. The experimental portion used capsules of PCM, with one U tube and various volumes of NPs and a capsule with two U tubes and the ideal amount of NPs. The thermal conductivity, melting time, and solidification time were improved with the addition of NPs, with 1% being the

ideal amount. Other higher amounts of NPs increased the viscosity, affecting the phase change times. The numerical simulation showed that the increased number of pipes decreased the melting time [15]. Farsani et al. [16] conducted a two-dimensional numerical study with RT 44HC paraffin and  $\text{Al}_2\text{O}_3$  NPs in a square with a square heat source in the center and four insulated walls. The effects of heat generation rate on flow and phase change were studied; then, the effects of NPs on the melting were studied. The Rayleigh number was varied to represent the heat generation rate, and it was found that the convection vortices that formed during melting were stronger with larger Rayleigh values. **Figure 3** shows the liquid fraction, average dimensionless temperature, maximum dimensionless temperature, and average Nusselt number during melting of the NePCM for a Rayleigh number of  $2.72 \times 10^6$ . It was concluded that NPs had little to no influence on the Nusselt number and temperature throughout the melting process (shown in **Figure 3**), and therefore, they did not recommended using NPs for enhancement [16]. The conclusions of this study differ from most studies. It is possible that this is due to the parameters tested in this study, as most other studies tested the effects of the dispersion of NPs on melting time or melting percentage in a certain amount of time, or thermal conductivity.

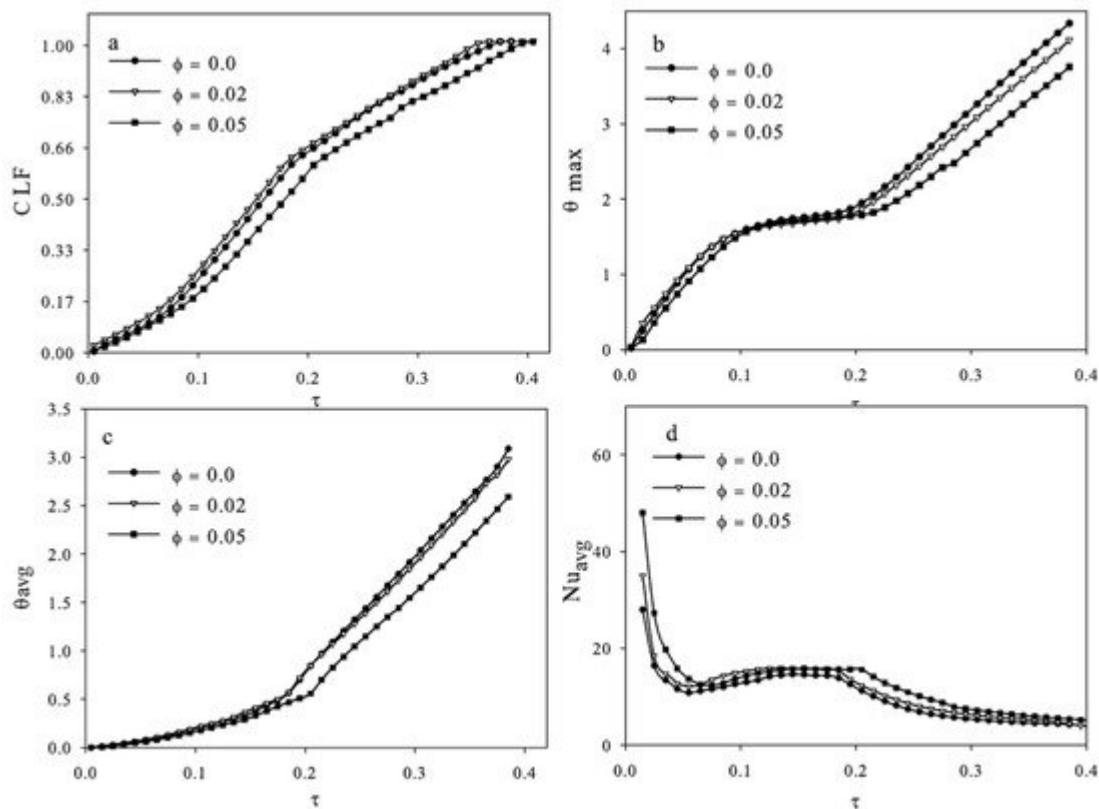


**Figure 3.** (a) liquid fraction, (b) average dimensionless temperature, (c) maximum dimensionless temperature, and (d) average Nusselt number in the Farsani et al. study (Copyright 2017 Elsevier) [16].

A 2017 numerical study by Elbahjaoui and El Qarnia used paraffin enhanced with  $\text{Al}_2\text{O}_3$  NPs in an LHTES system to investigate the effects of the aspect ratio of the PCM, volume fraction of the NPs, and the Reynolds and Rayleigh numbers on the thermal characteristics of the system. The enthalpy–porosity method was used to model melting. The study found that more NPs (higher volume fraction), a higher Rayleigh number, a higher aspect ratio,

and a higher Reynolds number all decreased the melting time. Increasing the Rayleigh number also increased the SHS. A correlation was written to find the melting time, and its results matched well with the numerical results [17].

### 2.1.3. Paraffin and Cu

In another study by Elbahjaoui and El Qarnia, a two-dimensional numerical was developed to study the solidification of n-octadecane PCM with copper NPs, which is another popular NP type. The LHTES system consisted of rectangular slabs of PCM with HTF sandwiched in between. The enthalpy–porosity method was used to simulate the phase change process to study the effects of the NP volume fraction, PCM aspect ratio, and HTF inlet temperature on the thermal performance of the LHTES system during the discharging process. Increasing the aspect ratio and decreasing the HTF inlet temperature both improved the performance of the system. The NPs also improved the solidification rate [18].

Another use of copper NPs with paraffin is reported in a numerical study by Nie et al. They investigated two different HTF injection orientations, top and bottom, for comparison. The PCM used was paraffin RT35 with pure copper NPs, and the HTF was water. Since the previous literature was conflicting, they first found that convection plays an important role in heat transfer for top-injected HTF. Heat flux was determined to be higher in the portion (top or bottom) that the HTF was injected from. The melting time was shorter for top injection when the thickness-to-height ratio was less than 0.05; however, it was longer when the ratio was larger than this. The effect of NP was less when the ratio was increased, and NP were more effective for bottom injection than top injection. The optimum thickness-to-height ratio was determined to be 0.05 [19]. Hosseini et al. numerically investigated the melting of another paraffin-based PCM, RT 50, with copper NPs. The effect of the NP volume fraction on the melting time, liquid fraction, and penetration length were studied. A shell-and-tube model was used with water as the HTF. They found that a higher volume fraction of NPs increased the liquid fraction and the penetration length of fluid, and it decreased the melting time [20]. Algarni et al. used NePCM to improve an evacuated tube solar collector system. They experimentally studied the effects of the paraffin PCM on the performance of the system, with and without the copper NPs. The experiment was conducted outdoors, with a pyranometer to test solar irradiation, thermocouples for temperature measurement, and a differential scanning calorimeter (DSC) to assess thermal properties. Without any PCM, the temperature of the system dropped steeply when the solar radiation decreased; however, with the addition of NePCM, the temperature decreased more gradually. The NePCM system had a 32% enhancement of efficiency overall. They minimized the agglomeration of particles with an ultrasonic vibrator. The system worked best with lower HTF mass flow rates of around 0.08 L/min. The NPs allowed for better storage on cloudy days than the non-NP storage [21]. Another study numerically modeled RT50 PCM enhanced with both Cu and Al<sub>2</sub>O<sub>3</sub> NPs in a concentric tube heat exchanger. The addition of the NPs enhanced melting and heat storage, which is an effect that decreased over time for the Al<sub>2</sub>O<sub>3</sub> particles. Due to an increase in the kinematic viscosity, there was a limit to the enhancement of NPs, since convection was suppressed if too many were added [22].

### 2.1.4. Paraffin with Carbons

Although metallic NPs are very effective, some tests with carbon-based NPs showed that they may be even more effective. Aqib et al. compared the effectiveness of paraffin enhanced with alumina (Al<sub>2</sub>O<sub>3</sub>) NP and nonmetallic



multiwall carbon nanotubes (MWCNTs) at three different concentrations. Mixtures contained either 2, 4, or 6 wt %. The mixtures were put through charging and discharging cycles with temperatures measured by thermocouples. As the concentration of particles increased, the heat transfer increased. The MWCNTs had higher peak temperatures than alumina NPs, making them the better option for enhancement [23]. Temel and Çiftçi went a step further than just comparing types, experimentally studying the effects of NPs type, size, and shape on the thermal properties of an NePCM. They used paraffin (A82) as the PCM and tested ZnO, TiO<sub>2</sub>, Al<sub>2</sub>O<sub>3</sub>, and MgO NPs as well as MWCNTs and graphene nanoplatelets (GNPs). They tested the particles using a scanning electron microscope (SEM) and the thermal properties using a DSC. The thermal conductivity improvements for MWCNTs, GNPs, ZnO, TiO<sub>2</sub>, Al<sub>2</sub>O<sub>3</sub>, and MgO were 26.7, 154.9, 2.6, 3.6, 6.5, and 8.4%, respectively, when added at 5% mass fraction. The differences in enhancements were due to the thermal conductivity of the particles and shape. For tests conducted only with Al<sub>2</sub>O<sub>3</sub> and MWCNTs, it was found that the increase in diameter led to an increase in thermal conductivity. NP types and mass fractions did not significantly change the melting and solidification temperatures. The melting times decreased in the same manner as the improvement in thermal conductivities, with ZnO showing the smallest improvement and the GNPs showing the greatest improvement [24].

Carbon NPs can even improve systems at incredibly small amounts. A 2018 study tested the melting and solidification of paraffin PCM with a melting range of 58–60 °C and MWCNTs. The specific heat of the NePCM was measured with DSC; then, the sample was melted and solidified, and resistance temperature detectors (RTDs) measured the temperatures. Melting times were lowest at 0.3 wt % MWCNTs, with a decrease of 30%, which was potentially due to increases in viscosity past this point. Solidification times were lowest at 0.9 wt %, with a decrease of 42.2% [25]. To test carbon NPs in a real-world scenario, Thalib et al. [26] conducted an experiment to test paraffin against graphene-enhanced paraffin in a tubular solar still (a device that desalinates water to provide potable fresh water). The experiments were conducted outdoors where the sun would provide the energy just as the device would be used. Peak temperatures of the systems throughout the day were above the 55 °C melting temperature, which were numbers that were higher with the addition of graphene into the PCM. The graphene enhanced the yield of fresh water that was produced compared to the other systems, since the heat absorbed was greater, meaning that during off hours, there was more heat stored up to release. The thermal and exergy efficiencies were also much higher with the NePCM [26].

However, not all studies found carbon NPs to be the most effective. Javadi et al. [27] studied Cu, CuO, Al<sub>2</sub>O<sub>3</sub>, TiO<sub>2</sub>, SiO<sub>2</sub>, multiwall carbon nanotubes, and graphene in paraffin using a three-dimensional numerical model. The NPs were tested in different shapes and volume fractions. Although all NPs enhanced the system, the best NP type was found to be Cu, while the worst was SiO<sub>2</sub>, as demonstrated by **Figure 4**. Then, Cu was tested at different volume fractions, and 0.2 was the ideal volume fraction to increase the thermal conductivity up to 55%. Cu was also tested in different shapes, and the “blade” shape (a long, thin, 3D ellipse-like shape) was the most efficient shape for enhancement when compared with spherical, brick, cylindrical, and platelet-shaped NPs [27].

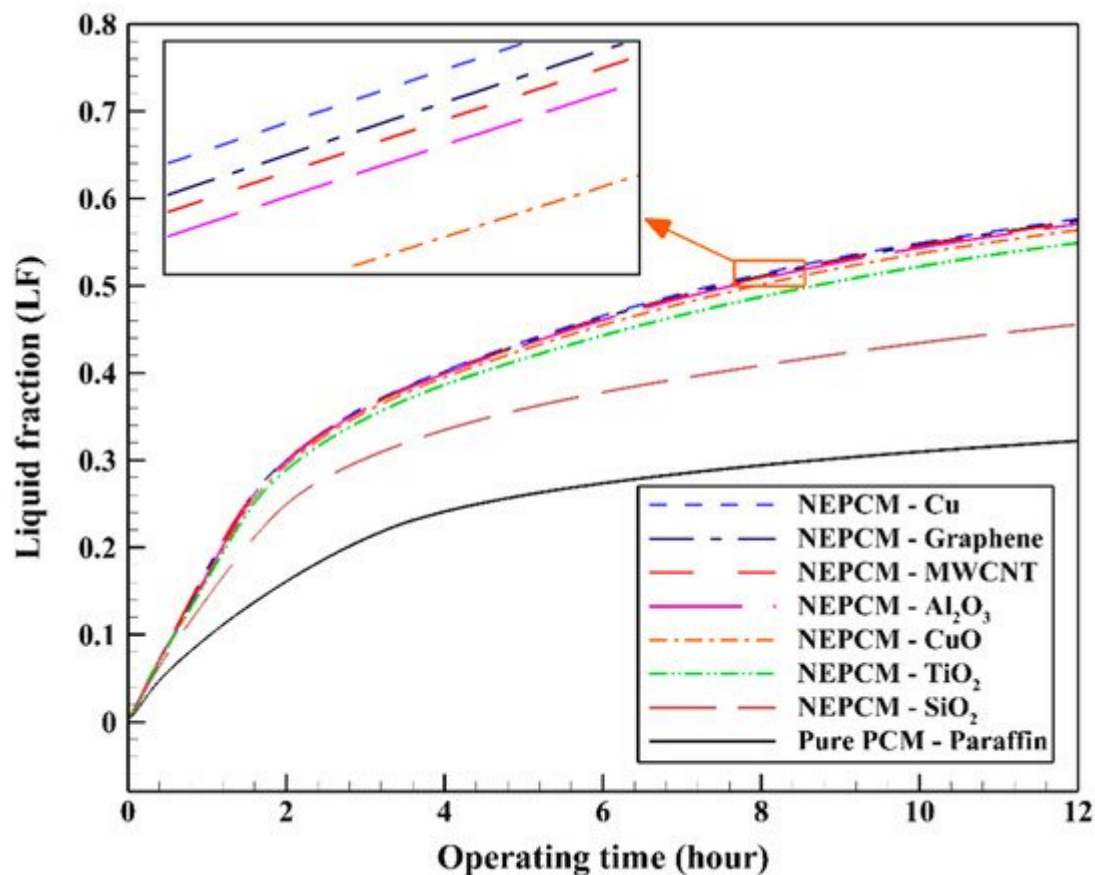


**Figure 4.** Liquid fractions of the different NePCMs tested over time by Javadi et al. (Copyright 2020 Javadi et al. <https://creativecommons.org/licenses/by/4.0/>) accessed on 18 June 2021 [27].

Similar to Javadi et al. [27], Bashar and Siddiqui [28] found MWCNTs to be less effective. Four different types of NPs were compared in an experimental study. Paraffin was used as the PCM with silver, copper oxide, aluminum oxide, and MWCNTs. The PCM was heated, and thermocouples were used for temperature measurements. All of the NPs enhanced the heat transfer; however, silver was the most effective, which was followed by copper oxide. Aluminum oxide and the MWCNT were much less effective because they sunk to the bottom of the PCM. Then, copper oxide was tested in varying mass fractions, 1, 3, 6, 8, and 10%, and it was found that the 6% mass fraction performed best [28].

### 2.1.5. Paraffin with Other NPs

A variety of metal oxide NPs were used to enhance RT82 PCM by Khatibi et al. [29] using a numerical study, including some of the ones above.  $\text{Al}_2\text{O}_3$ , ZnO, CuO, and  $\text{SiO}_2$  were added to the PCM to study the solidification process and test different HTF temperatures and tube diameters in three different LHTES units. The systems were a triplex-tube and two shell-and-tube, one with inner cooling and the other with outer cooling. The triplex tube system was modeled for all of the NP comparison studies; then, the different systems were compared, with and without NPs. All of the NPs reduced the solidification time, with  $\text{Al}_2\text{O}_3$  having the largest impact, which was followed by ZnO, CuO, and  $\text{SiO}_2$  in decreasing order, for a volume fraction of 0.02. For a volume fraction of 0.04, CuO had the greatest impact, which was followed by ZnO,  $\text{Al}_2\text{O}_3$ , and  $\text{SiO}_2$ , in that order. The decrease in solidification time



was caused by the increase in thermal conductivity and decrease in the latent heat of fusion. The triplex-tube system had the best performance, and external cooling the second best. The effect of the NPs was diminished with a decrease in HTF temperature and was also affected by the type of LHTES system [29].

Even though  $\text{SiO}_2$  NPs were found to be the least effective of those above, they can still be an effective enhancement. It may be that they work best at lower temperatures such as in the following system. Dastmalchi and Boyaghchi [30] used a numerical model to study a PCM–air heat exchanger with respect to exergy and cost per unit exergy for peak and off peak. The system worked along with an air conditioning system, using cool outdoor or indoor air to solidify PCM during off-peak times, and using the PCM to help cool the hot indoor air during peak times. The two-dimensional model was used to numerically perform an energy analysis, exergy analysis, and an exergoeconomic analysis. They simulated the temperatures of a typical week in late June in Esfahan, Iran. The PCM used was RT25 enhanced with  $\text{SiO}_2$  particles. Cooling power increased for low night temperatures and high day temperatures. Exergy efficiency was low during peak hours at higher indoor temperature setpoints. Setpoint ranges from 23 to 26 °C had the lowest cost and those from 24 to 25 °C had the highest cost with respect to exergy. The cost increased with increased slab length and with increased airflow due to the fan and compressor. Exergy efficiency increased at peak time and exergy destruction increased at off-peak time when NPs were added [30]. Pasupathi et al. [31] also found success with  $\text{SiO}_2$  when combined with  $\text{CeO}_2$ . They experimentally assessed the properties of paraffin PCM with hybrid  $\text{SiO}_2/\text{CeO}_2$  NPs at different mass percentages. At 2%, the particles begin to agglomerate, but they were evenly distributed up to that point. The NPs reduced the difference between the melting and solidification temperatures of the paraffin and delayed thermal decomposition. The thermal conductivity improved greatly up to 1% NPs and minimally above that percentage, as can be seen in **Figure 5**. It was concluded that 1% NPs was the best amount for enhancement [31].

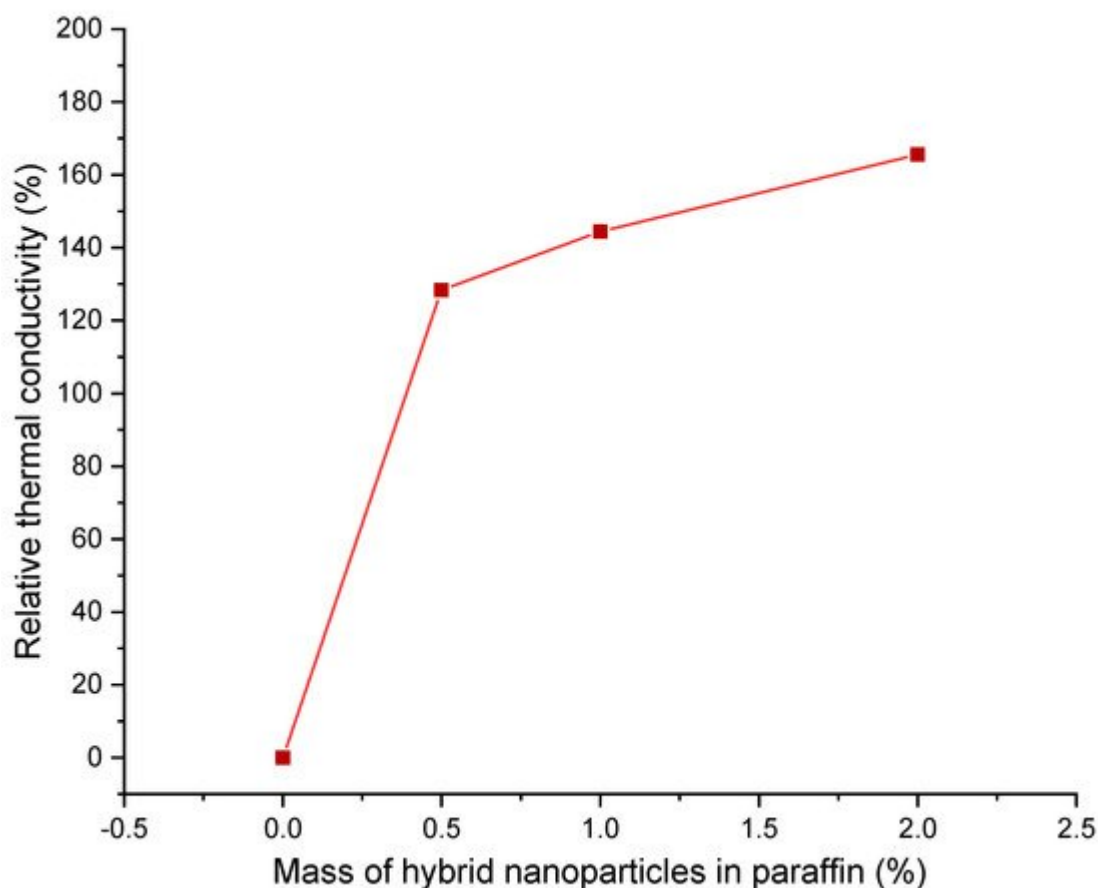


**Figure 5.** The relative enhancement in thermal conductivity with the addition of NPs (Copyright 2020 Pasupathi et al. <https://creativecommons.org/licenses/by/4.0/legalcode>) accessed on 18 June 2021 [31].

Another type of commonly used NP is plain aluminum. A study conducted by Zhou et al. [32] numerically and experimentally analyzed octadecane paraffin enhanced with aluminum NPs. Three-dimensional octadecane molecule models were created and made into a cubic unit cell, and aluminum was added into the unit cell. The non-equilibrium molecular dynamics method was used for the thermal conductivity simulation. The simulation showed that thermal conductivity increased with an increasing percentage of NPs; however, it increased more in the liquid PCM than the solid PCM. The experimental portion of the study used the transient thermal probe method to find thermal conductivity at room temperature (290 K) and at 320 K when the PCM is melted. The results showed that thermal conductivity increased with increase in aluminum particles. Comparing the two, the thermal conductivities followed the same trend, although the simulation values were smaller [32].

An interesting NP type was designed by Badakhsh et al. [33], who experimented with the melting and solidification of paraffin with aluminum nitride coated SiC (SiC@AlN) particles. SEM, laser diffraction, XRD, and DSC were used for characterization, among other methods. The effects of milling frequencies and the ball-to-powder mass ratio on the particle size distribution were tested: as the frequency increased, the particle diameter decreased. Thermal conductivity and specific heat testing by the transient plane source method showed that the SiC@AlN particles achieved higher thermal conductivity and lower specific heat than the other cases (plain paraffin, paraffin with AlN, paraffin with SiC). X-ray spectrometry showed that this was caused by the formation of conductive networks by the

SiC@AlN particles. An insignificant growth in latent heat was also observed, and the SiC@AlN particles were less expensive than AlN alone [33]. Another study with SiC particles also found them to be a promising enhancement. Maher et al. [34] compared two different nanomaterials in paraffin wax to improve thermal conductivity. After synthesis of the nanocomposites, they were characterized by a field emission SEM (Shown in **Figure 6**) as well as a DSC and laser flash apparatus, which was used to find thermal conductivity. The SiC-enhanced PCM had better thermal conductivity than the Ag-enhanced PCM, with the largest amount, 15 wt %, showing the best results. However, latent heat, melting temperature, and specific heat capacity were reduced by the NPs. This means that the highest weight percent is not always ideal, and the amount of NPs should be optimized on a case-by-case basis [34].

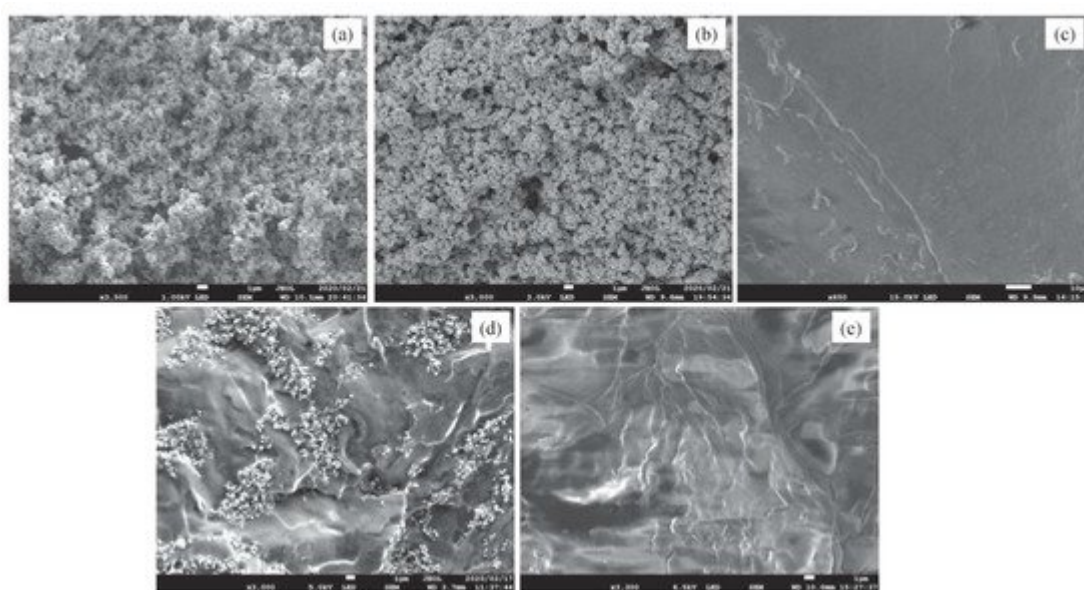


**Figure 6.** SEM images of (a) Silicon carbide, (b) Silver, (c) Pure paraffin wax, (d) Paraffin–SiC composite, and (e) Paraffin–Ag composite from Maher et al. (Copyright 2020 Elsevier) [34].

Ghalambaz et al. [35] numerically studied unspecified 2D hybrid NPs dispersed in a square of octadecane paraffin PCM. A “linearized correlation procedure” was used to find the properties of hybrid nanofluid to use in the simulations. They varied NP volume fraction, conductivity, and viscosity to test their effects. It was found that a large thermal conductivity and small viscosity resulted in shorter melting times. Initially, the mushy zone was thicker at the solid–liquid interface due to the lower convection there; however, over time, this phenomenon went away. A case study was also done with water and Ag-MgO NPs, which showed that these hybrid particles were more effective than plain MgO particles [35].

### 3.1.6. Eutectic Hydrate Salts

Other types of low-temperature PCMs are less commonly used; however, they can still have many benefits over water or paraffin. Liang and Chen [36] experimentally studied the solidification of eutectic hydrate salts with carbon NPs. Three samples with different amounts of thickeners were tested, showing an increase in onset and end temperatures from 0 to 3 wt %, but a decrease at 5 wt %. With increasing viscosity, the effects of the NPs

lessened, as did the absorption peak and phase change enthalpy, due to the decrease in micro-convection. Melting latent heat was decreased compared with ice and decreased with increased viscosity. The increase in viscosity also suppressed supercooling, decreased surface tension, and decreased the solidification time. Nucleating agents were proven to reduce or eliminate the degree of supercooling. Stability testing showed that after 20, 30, and 50 cycles, the supercooling reduced [36]. The salt hydrate Th29 was studied numerically by Jamalbadi et al. [37] as a heat sink for electronic circuits. The NePCM, which was enhanced with Cu NPs, was in a rectangular container next to a surface acoustic wave system. Three volume fractions were tested, and an increase in NP increased heat transfer at the solid–liquid interface. The NePCM improved the heat transfer by up to 10% [37].

## 2.2. NePCM and Fins

As discussed earlier, other heat transfer enhancement methods are commonly combined with NePCM to provide further enhancement of the LHTES system. NePCM, unlike some other enhancement methods, can be combined with nearly any type of enhancement due to the size of the particles. The following studies assessed NePCM with fins.

Hosseinzadeh et al. [38] numerically studied the enhancement of an LHTES system with branching or rectangular fins and  $\text{MoS}_2\text{-TiO}_2$  NPs in water as the NePCM. The system was studied with each enhancement individually and with NPs and fins together. The tree-like fins provided better results than the rectangular fins and no fins. The inclusion of NPs without fins showed that the NPs did improve the system; however, they did not show as much of an improvement as the fins. Together, the best option for improving performance was the NPs of the highest concentration, along with the branched fins. This was significantly better than NPs alone and slightly better than branched fins alone [38].

Hajizadeh et al. [39] also studied the combination of NePCM and branched fins. The numerical study focused on the solidification of RT35 enhanced by Y-fins and CuO NPs in three different cases. The cases were no fins (case one), long Y-fins on top and V-fins on bottom (case two), and V-fins on top with Y-fins on bottom (case three), as shown in **Figure 7**. The first case was tested with two volume fractions of nanofluid, and the second and third were tested with and without NPs. The system without fins was the least efficient, and case two was more efficient than case three. As a result of buoyancy effects, case two was also more affected by the NP dispersion than case three. The amount of energy decreased with an increase of NPs, but case two stored more energy than case three [39].

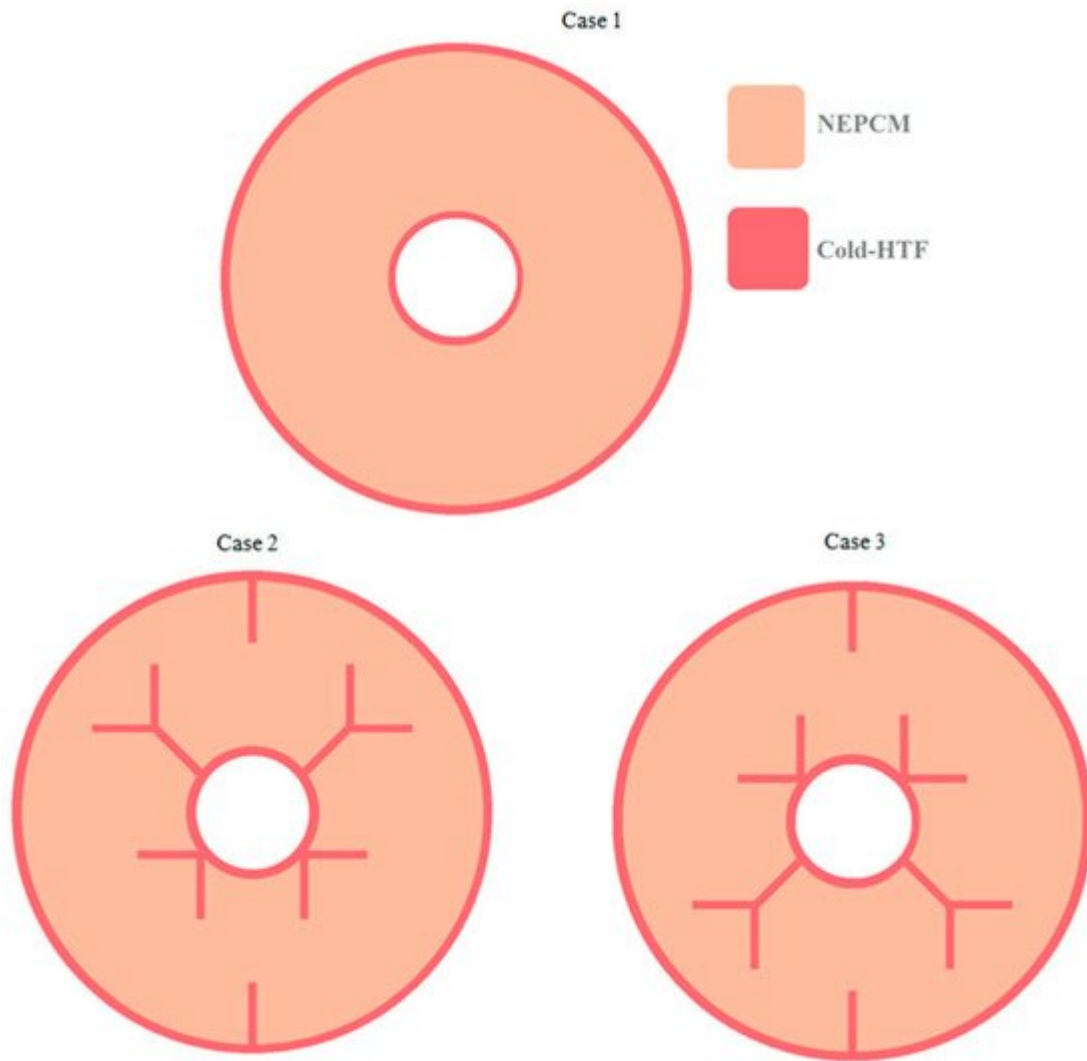


**Figure 7.** Fin configurations for the three cases studied by Hajizadeh et al. (Copyright 2020 Elsevier) [39].

CuO seems to be a popular choice for NPs when combined with fins. Nakhci et al. [40] studied stair-shaped fins and CuO NPs in an LHTES system with lauric acid PCM. No difference was found for the orientation of the fins (upward or downward stairs) early on; however, later in melting, natural convection affected the two orientations differently. Overall, the downward stair fins had a shorter melting time due to more uniform temperatures. More fins reduced the melting time but also reduced the total storage capacity, and the same resulted from thicker fins. NPs along with fins improved the melting performance. Smaller stair ratios caused initially faster melting but slower melting later. An increased stair ratio improved the energy storage capacity [40]. Copper oxide particles were chosen also by Li et al. [41], who examined the charging process of paraffin PCM with different sizes and configurations of Y-shaped fins. Six different cases of fins were studied. As is demonstrated in **Figure 8**, the fourth case, with long, thin fins alternating attachment to the outer and inner wall, was the best case. The worst case was case one, with short fins attached only to the inner wall. Longer, thinner fins allowed for natural convection, accelerating the melting [41].



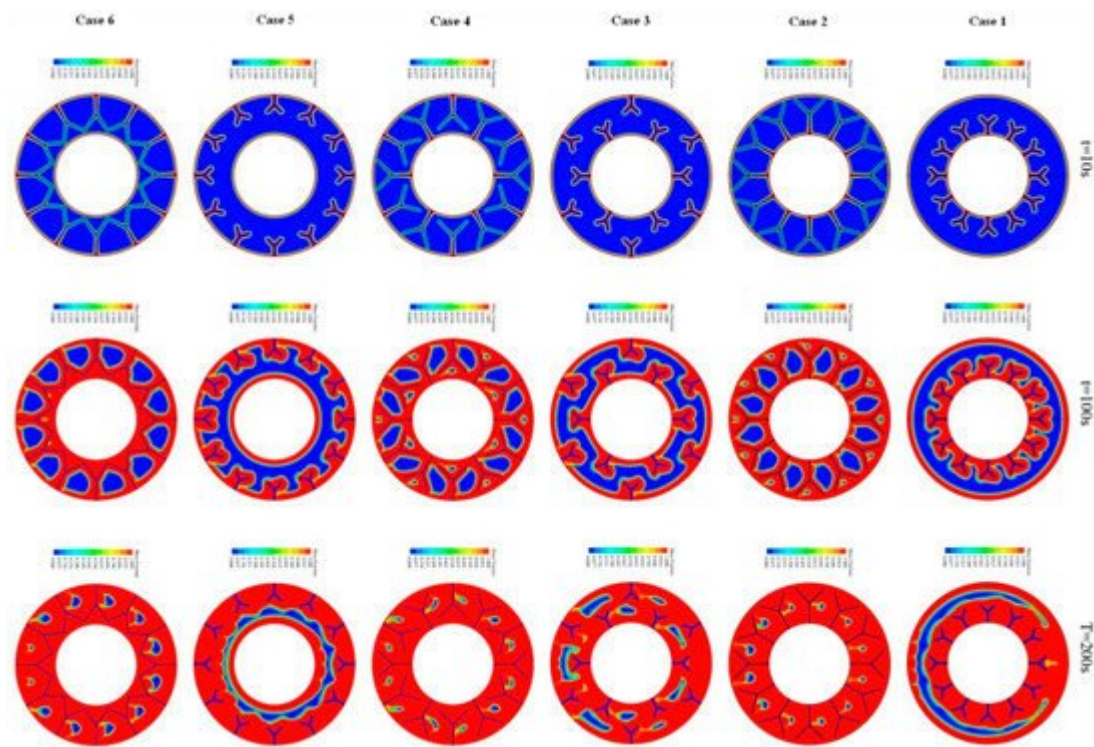


**Figure 8.** The liquid fraction in the six different cases at different times. (Copyright 2020 Elsevier) [42].

Instead of rectangular or branched fins, Ren et al. [43] numerically studied the effects of using triangular fins, along with copper NPs, as enhancements for N-eicosane PCM. The two triangle fins were compared with one rectangle fin with the same total volume, which showed that the triangle fins melted more PCM under the same conditions. Comparing different fin lengths, longer fins improved the system, and triangle fins of each length were better than their rectangular counterparts. The melting rate was also improved by the addition of NPs, with greater concentrations producing better results, although the pure PCM with triangle fins was still better than the NePCM with a rectangular fin. However, the greater the percentage of NPs, the less of a difference there was between the two types of fins. NePCM was further studied with the triangular fins, which showed that the long, narrow fins with unequal lengths (longer on bottom and shorter on top, to enhance convection on top and conduction on the bottom) greatly improved the NePCM melting rate [43].

Copper fins are also a popular choice, even with other types of NPs. Mahdi et al. [44] used a triplex tube heat exchanger for the simultaneous charging and discharging of PCM, with an outer tube of cold HTF, a middle tube of RT82 PCM with copper fins extending into it, and an inner tube of hot HTF. Simultaneous charging and discharging is a likely real-world scenario that is not often studied. They numerically studied different fin setups and enhancement with  $\text{Al}_2\text{O}_3$  for the system. Adding fins caused natural convection to assist in melting the bottom half of the PCM, where without fins, natural convection would only occur in the top half. Adding V-shaped fins in the bottom half also improved melting. Since it simultaneously charged and discharged, optimization was based on the final steady-state time and final steady-state liquid fraction of the system. NPs provided very little enhancement to the system in comparison to the fins, so they were considered to be unnecessary [44]. Bondareva et al. [42] also used copper fins and alumina NPs to enhance the thermal performance of an LHTES system. They tested various



PCMs with NPs and fins as heat sinks for electronics. The rectangular, two-dimensional numerical model with copper fins was heated by a constant source underneath. The liquid volume fraction versus time for the five PCMs tested (n-octadecane, capric acid, lauric acid, RT-50, and RT-80) is shown in **Figure 9**. Since n-octadecane has the lowest melting point, it started melting first; however, since it melted quickly, it only cooled for a short amount of time. The lauric acid had the lowest temperature heat sink after four minutes, making it the best choice. NPs reduced latent heat, accelerated the melting process, and reduced the overall heat capacity. As a result of this, NPs only enhanced the system up to 2% concentration, which was determined to be the best concentration [42].

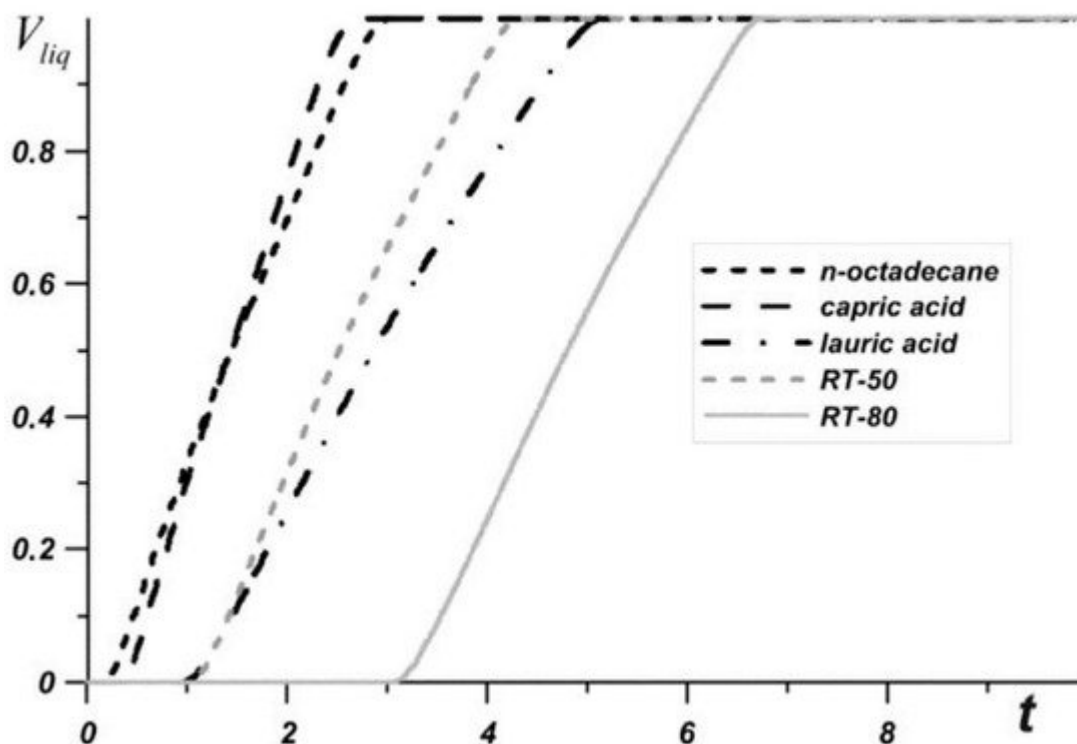


**Figure 9.** Liquid volume fraction over time for the different PCMs tested by Bondareva et al. (Copyright 2020 Bondareva et al. <https://creativecommons.org/licenses/by/4.0/legalcode>) Accessed on 18 June 2021 [42].

Copper and copper oxide seem to be very common and effective materials for fin–NP enhanced LHTES systems. What is lacking is combinations of other fin and NP materials. Some studies also found that in comparison to fins, the NPs were an unnecessary enhancement. This was not the case with all of the studies, and perhaps it was due to the type of NP used in combination with the PCM and melting temperature of the system. Further studies of those systems with other NP materials could be conducted. Additionally, there seems to be a lack of middle and high temperature studies with NPs and fins as well as a lack of experimental studies. A majority—if not all—of these studies with NPs and fins are conducted numerically. Experimental studies should be conducted in the future. **Table 1** summarizes the studies that used NePCM combined with fins to enhance LHTES system.

**Table 1.** A summary of studies that used NePCM combined with fins to enhance LHTES system.

Authors	PCM Melting Point (°C)	Nanoparticle Type/Enhancement Method(s)	Phase Change Process	Study Case	Result
Hosseinzadeh et al. (2021) [38]	Water (0 °C) Low	MoS <sub>2</sub> -TiO <sub>2</sub> and branched fins	Solidification	Numerical (2D)	High NP concentration with branched fins were the best enhancement technique
Hajizadeh et al. (2020) [39]	RT35 (35 °C) Low	CuO and branched fins	Solidification	Numerical (2D)	NP improved all cases, case 2 worked best
Nakhachi et al. (2021) [40]	Lauric acid (43.4–48.1 °C) Low	CuO and stair fins	Melting	Numerical (2D)	NP and stair fins improved melting
Li et al. (2021) [41]	Paraffin (n-octadecane) Low	Copper oxide and fins	Melting	Numerical (2D)	Long, thin fins from both walls worked best
Ren et al. (2019) [43]	N-eicosane (35.85 °C) Low	Copper and triangle fins	Melting	Numerical (2D)	Triangle fins and NP improved system
Mahdi et al. (2019) [44]	RT82 (77–85 °C) Low	Al <sub>2</sub> O <sub>3</sub> and copper fins	Simultaneous charging and discharging	Numerical (2D)	Fins and their geometry had greater effects than the NPs
Bondareva et al. (2020) [42]	n-Octadecane (28.05 °C), Capric acid (32 °C), Lauric acid (46 °C), RT-50 (49 °C), RT-80 (81 °C) Low	Al <sub>2</sub> O <sub>3</sub> and fins	Melting	Numerical (2D)	NPs enhanced up to 2% concentration

## References

1. Sarbu, I.; Sebarchievici, C. A comprehensive review of thermal energy storage. Sustainability 2018, 10, 191.
2. De Gracia, A.; Cabeza, L.F. Phase change materials and thermal energy storage for buildings. Energy Build. 2015, 103, 414–419.

3. Khan, Z.; Khan, Z.; Ghafoor, A. A review of performance enhancement of PCM based latent heat storage system within the context of materials, thermal stability and compatibility. *Energy Convers. Manag.* 2016, 115, 132–158.
4. Tiari, S.; Qiu, S. Three-dimensional simulation of high temperature latent heat thermal energy storage system assisted by finned heat pipes. *Energy Convers. Manag.* 2015, 105, 260–271.
5. Jiang, Z.Y.; Qu, Z.G. Lithium-ion battery thermal management using heat pipe and phase change material during discharge–charge cycle: A comprehensive numerical study. *Appl. Energy* 2019, 242, 378–392.
6. Tariq, S.L.; Ali, H.M.; Akram, M.A.; Janjua, M.M.; Ahmadlouydarab, M. Nanoparticles enhanced phase change materials (NePCMs)-A recent review. *Appl. Therm. Eng.* 2020, 176, 115305.
7. European Energy Research Alliance. High-Temperature Latent Heat Storage [digital]; EERA: Brussels, Belgium, 2018; Available online: (accessed on 18 June 2021).
8. Huang, Z.; Xie, N.; Luo, Z.; Gao, X.; Fang, X.; Fang, Y.; Zhang, Z. Characterization of medium-temperature phase change materials for solar thermal energy storage using temperature history method. *Sol. Energy Mater. Sol. Cells* 2018, 179, 152–160.
9. Elgafy, A.; Lafdi, K. Effect of carbon nanofiber additives on thermal behavior of phase change materials. *Carbon* 2005, 43, 3067–3074.
10. Khodadadi, J.M.; Hosseinizadeh, S.F. Nanoparticle-enhanced phase change materials (NEPCM) with great potential for improved thermal energy storage. *Int. Commun. Heat Mass Transf.* 2007, 34, 534–543.
11. Jourabian, M.; Farhadi, M. Melting of nanoparticles-enhanced phase change material (NEPCM) in vertical semicircle enclosure: Numerical study. *J. Mech. Sci. Technol.* 2015, 29, 3819–3830.
12. Feng, Y.; Li, H.; Li, L.; Bu, L.; Wang, T. Numerical investigation on the melting of nanoparticle-enhanced phase change materials (NEPCM) in a bottom-heated rectangular cavity using lattice Boltzmann method. *Int. J. Heat Mass Transf.* 2015, 81, 415–425.
13. Akhmetov, B.; Navarro, M.E.; Seitov, A.; Kaltayev, A.; Bakenov, Z.; Ding, Y. Numerical study of integrated latent heat thermal energy storage devices using nanoparticle-enhanced phase change materials. *Sol. Energy* 2019, 194, 724–741.
14. Abdulateef, A.M.; Jaszczur, M.; Hassan, Q.; Anish, R.; Niyas, H.; Sopian, K.; Abdulateef, J. Enhancing the melting of phase change material using a fins–nanoparticle combination in a triplex tube heat exchanger. *J. Energy Storage* 2021, 35, 102227.
15. Zaidan, M.J.; Alhamdo, M.H. Improvement in heat transfer inside a phase change energy system. *Int. J. Mech. Mechatron. Eng.* 2018, 18, 33–46.

16. Farsani, R.Y.; Raisi, A.; Nadooshan, A.A.; Vanapalli, S. Does nanoparticles dispersed in a phase change material improve melting characteristics? *Int. Commun. Heat Mass Transf.* 2017, 89, 219–229.
17. Elbahjaoui, R.; el Qarnia, H. Transient behavior analysis of the melting of nanoparticle-enhanced phase change material inside a rectangular latent heat storage unit. *Appl. Therm. Eng.* 2017, 112, 720–738.
18. Elbahjaoui, R.; el Qarnia, H. Thermal analysis of nanoparticle-enhanced phase change material solidification in a rectangular latent heat storage unit including natural convection. *Energy Build.* 2017, 153, 1–17.
19. Nie, C.; Liu, J.; Deng, S. Effect of geometric parameter and nanoparticles on PCM melting in a vertical shell-tube system. *Appl. Therm. Eng.* 2021, 184, 116290.
20. Hosseini, S.M.J.; Ranjbar, A.A.; Sedighi, K.; Rahimi, M. Melting of nanoparticle-enhanced phase change material inside shell and tube heat exchanger. *J. Eng.* 2013, 2013, 1–8.
21. Algarni, S.; Mellouli, S.; Alqahtani, T.; Almutairi, K.; Khan, A.; Anqi, A. Experimental investigation of an evacuated tube solar collector incorporating nano-enhanced PCM as a thermal booster. *Appl. Therm. Eng.* 2020, 180, 115831.
22. Nitsas, M.T.; Koronaki, I.P. Thermal analysis of pure and nanoparticle-enhanced PCM—Application in concentric tube heat exchanger. *Energies* 2020, 13, 3841.
23. Aqib, M.; Hussain, A.; Ali, H.M.; Naseer, A.; Jamil, F. Experimental case studies of the effect of Al<sub>2</sub>O<sub>3</sub> and MWCNTs nanoparticles on heating and cooling of PCM. *Case Stud. Therm. Eng.* 2020, 22, 100753.
24. Temel, Ü.N.; Çiftçi, B.Y. Determination of thermal properties of a82 organic phase change material embedded with different type nanoparticles. *Farklı Tipler Nanoparçacıklarla Katkılanan A82 Organik Faz Değiştiren Malzemenin Termal Özelliklerinin Belirlenmesi* 2018, 38, 75–85.
25. Murugan, P.; Ganesh Kumar, P.; Kumaresan, V.; Meikandan, M.; Malar Mohan, K.; Velraj, R. Thermal energy storage behaviour of nanoparticle enhanced PCM during freezing and melting. *Phase Transit.* 2018, 91, 254–270.
26. Thalib, M.M.; Manokar, A.M.; Essa, F.A.; Vasimalai, N.; Sathyamurthy, R.; Garcia Marquez, F.P. Comparative study of tubular solar stills with phase change material and nano-enhanced phase change material. *Energies* 2020, 13, 3989.
27. Javadi, H.; Urchueguia, J.F.; Mousavi Ajarostaghi, S.S.; Badenes, B. Numerical study on the thermal performance of a single U-tube borehole heat exchanger using nano-enhanced phase change materials. *Energies* 2020, 13, 5156.

28. Bashar, M.; Siddiqui, K. Experimental investigation of transient melting and heat transfer behavior of nanoparticle-enriched PCM in a rectangular enclosure. *J. Energy Storage* 2018, 18, 485–497.
29. Khatibi, M.; Nemati-Farouji, R.; Taheri, A.; Kazemian, A.; Ma, T.; Niazmand, H. Optimization and performance investigation of the solidification behavior of nano-enhanced phase change materials in triplex-tube and shell-and-tube energy storage units. *J. Energy Storage* 2021, 33, 102055.
30. Dastmalchi, M.; Boyaghchi, F.A. Exergy and economic analyses of nanoparticle-enriched phase change material in an air heat exchanger for cooling of residential buildings. *J. Energy Storage* 2020, 32, 101705.
31. Pasupathi, M.K.; Alagar, K.; Stalin P, M.J.; Matheswaran, M.M.; Aritra, G. Characterization of hybrid-nano/paraffin organic phase change material for thermal energy storage applications in solar thermal systems. *Energies* 2020, 13, 5079.
32. Zhou, Y.; Jiang, Y.; Liu, F.; Li, Q. Thermal conductivity and thermal mechanism of aluminum nanoparticles/octadecane composite phase change materials from molecular dynamics simulations and experimental study. *J. Ovonic Res.* 2016, 12, 49–58.
33. Badakhsh, A.; An, K.-H.; Park, C.W.; Kim, B.-J. Effects of biceramic AlN-SiC microparticles on the thermal properties of paraffin for thermal energy storage. *J. Nanomater.* 2018, 2018, 1–10.
34. Maher, H.; Rocky, K.A.; Bassiouny, R.; Saha, B.B. Synthesis and thermal characterization of paraffin-based nanocomposites for thermal energy storage applications. *Therm. Sci. Eng. Prog.* 2021, 22, 100797.
35. Ghalambaz, M.; Doostani, A.; Chamkha, A.J.; Ismael, M.A. Melting of nanoparticles-enhanced phase-change materials in an enclosure: Effect of hybrid nanoparticles. *Int. J. Mech. Sci.* 2017, 134, 85–97.
36. Liang, L.; Chen, X. Preparation and thermal properties of eutectic hydrate salt phase change thermal energy storage material. *Int. J. Photoenergy* 2018, 2018, 1–9.
37. Jamalabadi, M.Y.A. Use of nanoparticle enhanced phase change material for cooling of surface acoustic wave sensor. *Fluids* 2021, 6, 31.
38. Hosseinzadeh, K.; Erfani Moghaddam, M.A.; Asadi, A.; Mogharrebi, A.R.; Jafari, B.; Hasani, M.R.; Ganji, D.D. Effect of two different fins (longitudinal-tree like) and hybrid nano-particles (MoS<sub>2</sub>-TiO<sub>2</sub>) on solidification process in triplex latent heat thermal energy storage system. *Alex. Eng. J.* 2021, 60, 1967–1979.
39. Hajizadeh, M.R.; Keshteli, A.N.; Bach, Q.-V. Solidification of PCM within a tank with longitudinal-Y shape fins and CuO nanoparticle. *J. Mol. Liq.* 2020, 317, 114188.
40. Nakhchi, M.E.; Hatami, M.; Rahmati, M. A numerical study on the effects of nanoparticles and stair fins on performance improvement of phase change thermal energy storages. *Energy* 2021,

215, 119112.

41. Li, F.; Almarashi, A.; Jafaryar, M.; Hajizadeh, M.R.; Chu, Y.-M. Melting process of nanoparticle enhanced PCM through storage cylinder incorporating fins. *Powder Technol.* 2021, 381, 551–560.
42. Bondareva, N.S.; Gibanov, N.S.; Sheremet, M.A. Computational study of heat transfer inside different PCMs enhanced by Al<sub>2</sub>O<sub>3</sub> nanoparticles in a copper heat sink at high heat loads. *Nanomaterials* 2020, 10, 284.
43. Ren, Q.; Xu, H.; Luo, Z. PCM charging process accelerated with combination of optimized triangle fins and nanoparticles. *Int. J. Therm. Sci.* 2019, 140, 466–479.
44. Mahdi, J.M.; Lohrasbi, S.; Ganji, D.D.; Nsofor, E.C. Simultaneous energy storage and recovery in the triplex-tube heat exchanger with PCM, copper fins and Al<sub>2</sub>O<sub>3</sub> nanoparticles. *Energy Convers. Manag.* 2019, 180, 949–961.

---

Retrieved from <https://encyclopedia.pub/entry/history/show/27748>